Electronic Supplementary Material (ESI) for Journal of Materials Chemistry A.

Supporting Information

Hollow nickel-coated silica microspheres containing rhodium nanoparticles for highly selective production of hydrogen from hydrous hydrazine

Jung Bo Yoo, Han Sol Kim, Seung Hee Kang, Byeongno Lee, and Nam Hwi Hur*

Department of Chemistry, Sogang University, Seoul 121-742, Korea.

*e-mail: nhhur@sogang.ac.kr

Table of Contents

I. Synthesis of Rh-embedded core/shell silica microspheres (Rh@SiO_2).

Core/shell SiO_2 microspheres (0.25 g) with core diameters of ~300 nm and the shell thicknesses ranging from 20 to 30 nm were dispersed in 50 mL of ethanol in a 100 mL round-bottom flask. The core/shell silica microspheres were used as supports for embedding rhodium nanoparticles (NPs). Detailed procedures are described in our previous report.[1] The solution was sonicated for 1 h to disperse the core/shell silica microspheres without agglomeration followed by dropwise addition of 0.2 mL of 3-aminopropyltrimethoxy-silane (APTMS). The reaction mixture was then vigorously stirred for 6 h at 50 ^{o}C to bind the APTMS molecules onto the surfaces of the silica microspheres. The amine-functionalized silica microspheres were purified by centrifuging the microspheres, discarding the supernatant, and re-dispersing the microspheres in ethanol. To load Rh into the microspheres, rhodium chloride hydrate (0.04 g, 1.9×10^{-4} mol) in 10 mL of distilled water was added to the functionalized silica microspheres in 40 mL of ethanol, and the mixture was stirred for 12 h at room temperature. The reaction yielded a light violet solution, indicating the deposition of Rh NPs on the silica surface. After centrifuging the solution, the supernatant was discarded and the microspheres were washed twice with ethanol. The Rh-loaded silica microspheres were dried in an oven at 100 ^{o}C and annealed at 750 ^{o}C for 20 h under a reducing atmosphere (Ar/H_2 = 95:5) to yield Rh-embedded microspheres (Rh@SiO_2.).

II. Tables

Table S1. EDX elemental and ICP-AES analyses results for $Rh/Ni(OH)_2@SiO_2$-1T, $Rh/Ni(OH)_2@SiO_2$-2T, and $Rh/Ni(OH)_2@SiO_2$-3T. ICP-AES data are in round brackets.

Element	Ni wt %	Rh wt %	Si wt %	O wt %
$Rh/Ni(OH)_2@SiO_2$-1T	26.71 (26.64)	2.66 (2.70)	48.32 (33.01)	22.31 (37.63)
$Rh/Ni(OH)_2@SiO_2$-2T	31.81 (31.14)	3.65 (4.32)	32.95 (30.12)	31.59 (34.42)
$Rh/Ni(OH)_2@SiO_2$-3T	45.38 (44.20)	5.20 (6.36)	21.89 (23.07)	27.53 (26.36)

Table S2. Catalytic activities of various alloy catalysts for the H_2 production from hydrous hydrazine

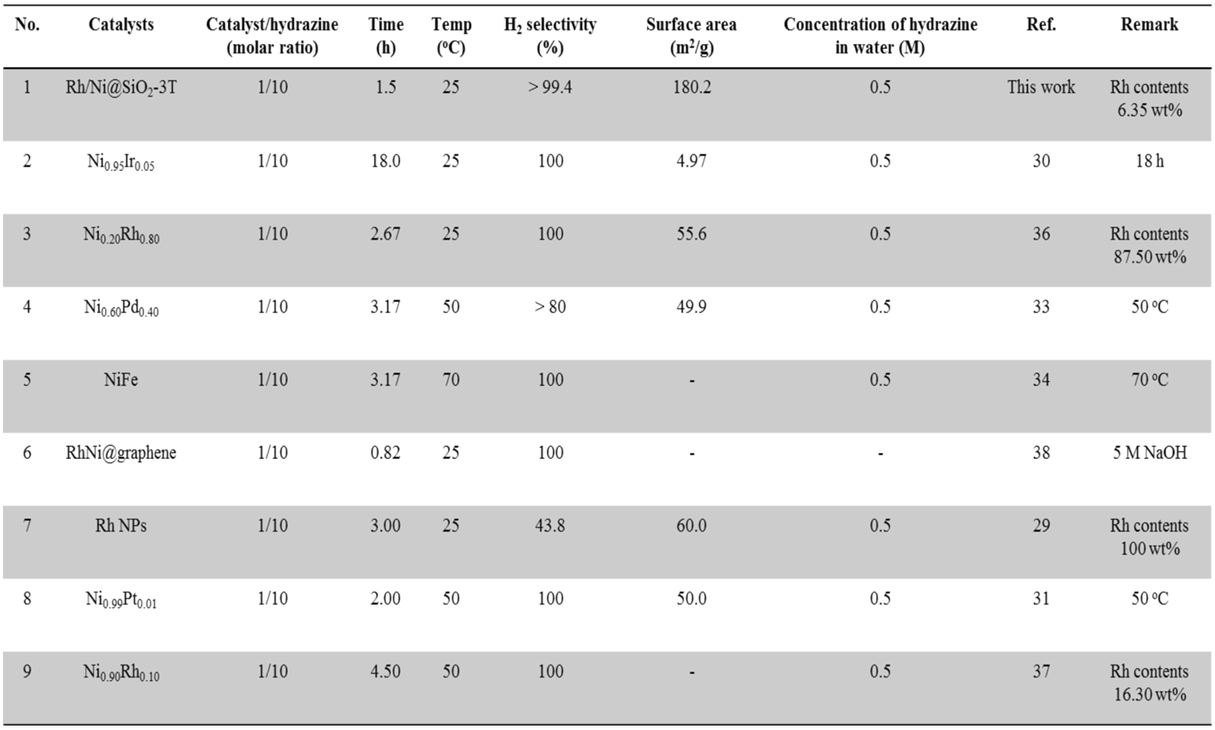

No.	Catalysts	Catalyst/hydrazine (molar ratio)	Time (h)	Temp (°C)	H_2 selectivity (%)	Surface area (m^2/g)	Concentration of hydrazine in water (M)	Ref.	Remark
1	$Rh/Ni@SiO_2$-3T	1/10	1.5	25	> 99.4	180.2	0.5	This work	Rh contents 6.35 wt%
2	$Ni_{0.95}Ir_{0.05}$	1/10	18.0	25	100	4.97	0.5	30	18 h
3	$Ni_{0.20}Rh_{0.80}$	1/10	2.67	25	100	55.6	0.5	36	Rh contents 87.50 wt%
4	$Ni_{0.60}Pd_{0.40}$	1/10	3.17	50	> 80	49.9	0.5	33	50 °C
5	NiFe	1/10	3.17	70	100	-	0.5	34	70 °C
6	RhNi@graphene	1/10	0.82	25	100	-	-	38	5 M NaOH
7	Rh NPs	1/10	3.00	25	43.8	60.0	0.5	29	Rh contents 100 wt%
8	$Ni_{0.99}Pt_{0.01}$	1/10	2.00	50	100	50.0	0.5	31	50 °C
9	$Ni_{0.90}Rh_{0.10}$	1/10	4.50	50	100	-	0.5	37	Rh contents 16.30 wt%

III. Figures

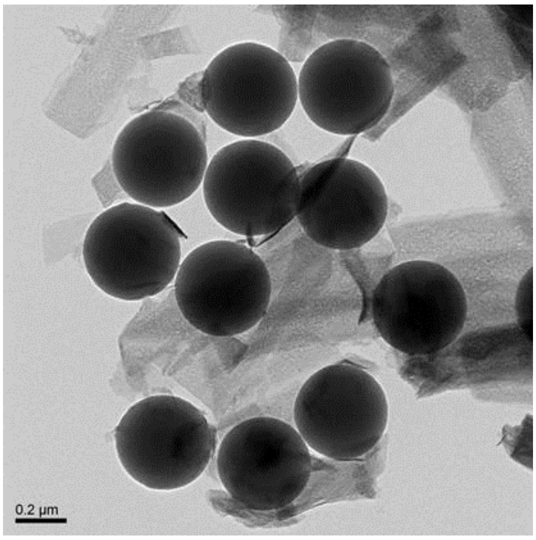

Fig. S1 Representative TEM image of Ni-coated microspheres prepared using core SiO_2 microspheres as templates instead of core/shell SiO_2 microspheres. The microspheres were synthesized via the procedure used for the synthesis of $Ni(OH)_2@SiO_2$ microspheres.

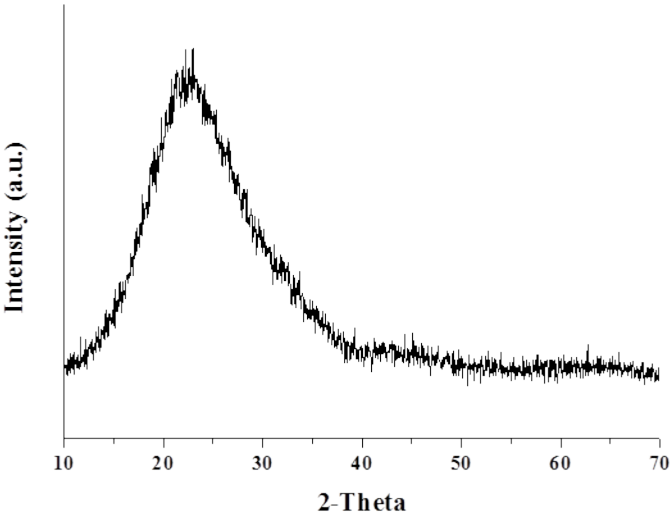

Fig. S2 Powder XRD patterns of $Rh/Ni(OH)_2@SiO_2$. A very broad peak at ~20° is due to SiO_2.

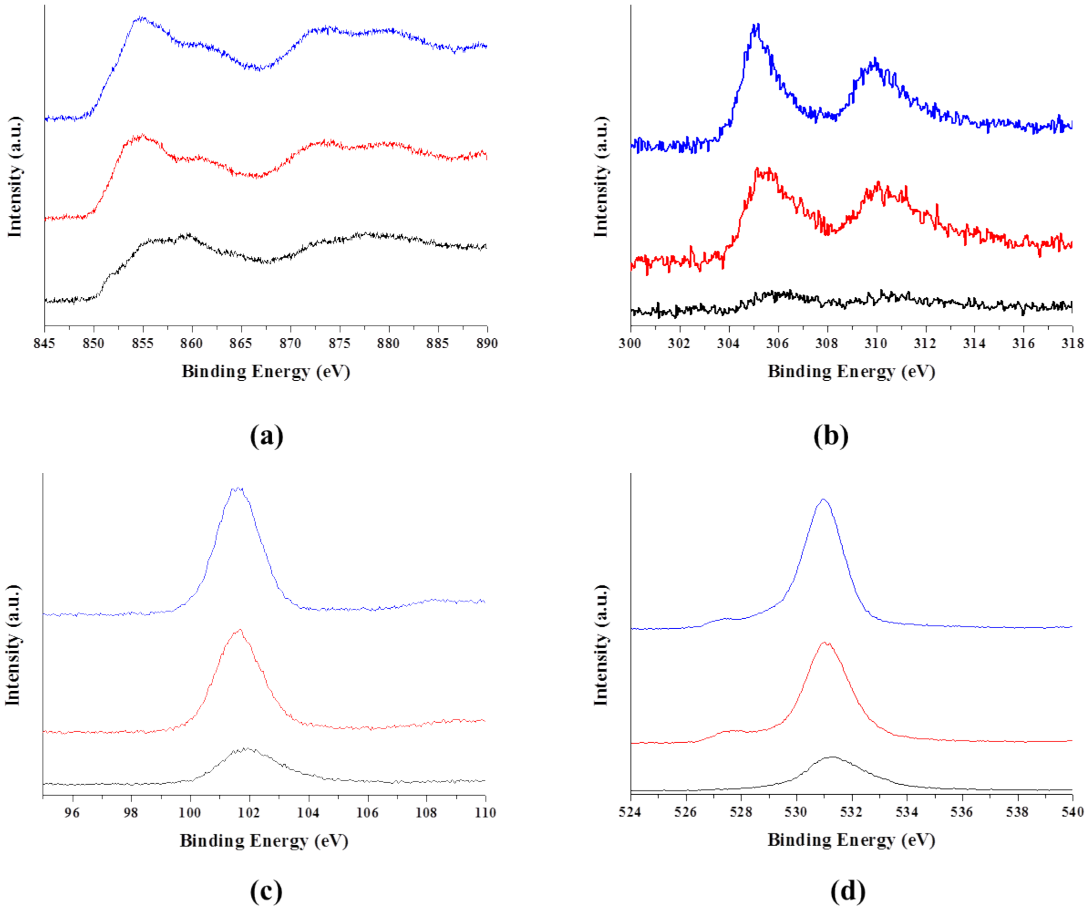

(a) **(b)**

(c) **(d)**

Fig. S3 XPS data for Rh/Ni@SiO$_2$-1T (black line), Rh/Ni@SiO$_2$-2T (red line), and Rh/Ni@SiO$_2$-3T (blue line) in the regions of (a) Ni 2*p*, (b) Rh 3*d*, (c) Si 2*p*, and (d) O 1*s*.

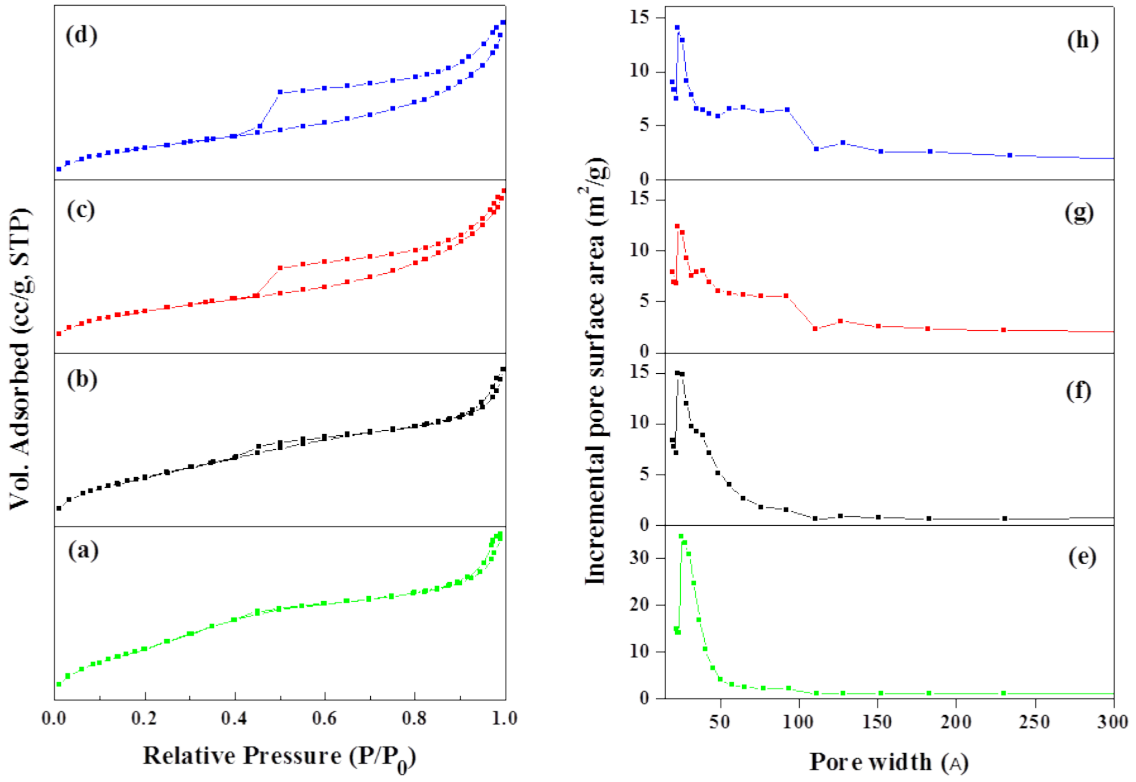

Fig. S4 Nitrogen adsorption and desorption isotherms of (a) core/shell SiO_2, (b) Rh/Ni@SiO_2-1T, (c) Rh/Ni@SiO_2-2T, and (d) Rh/Ni@SiO_2-3T. The pore-size distributions of (e) core/shell SiO_2, (f) Rh/Ni@SiO_2-1T, (g) Rh/Ni@SiO_2-2T, and (h) Rh/Ni@SiO_2-3T were calculated using the Barrett-Joyner-Halenda method; the average pore widths of core/shell SiO_2, Rh/Ni@SiO_2-1T, Rh/Ni@SiO_2-2T, and Rh/Ni@SiO_2-3T were 4.3 nm, 4.7 nm, 5.4 nm, and 5.6 nm, respectively.

Fig. S5 Rh/Ni@SiO$_2$-3T microspheres were separated after the catalytic reactions using a permanent magnet. They were recovered and reused as catalysts.

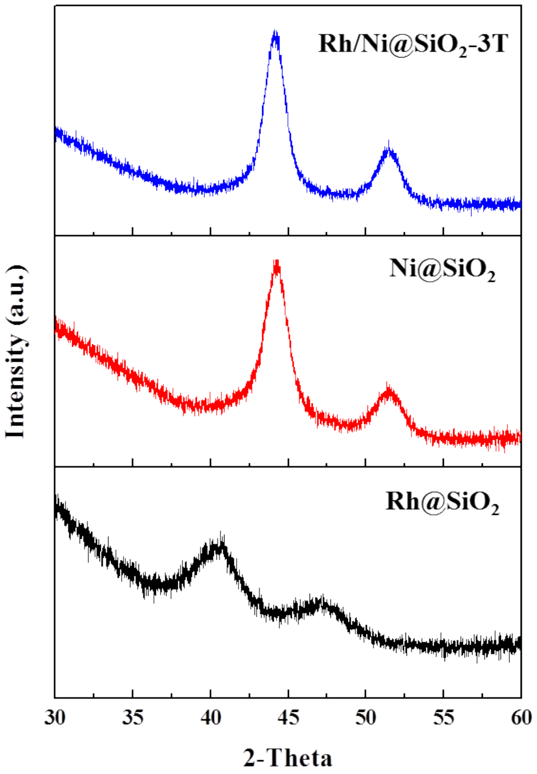

Fig. S6 Powder XRD patterns of Rh@SiO$_2$, Ni@SiO$_2$, and Rh/Ni@SiO$_2$-3T. The intensities of Rh@SiO$_2$ are very weak compared to those of Ni@SiO$_2$ and Rh/Ni@SiO$_2$-3T.

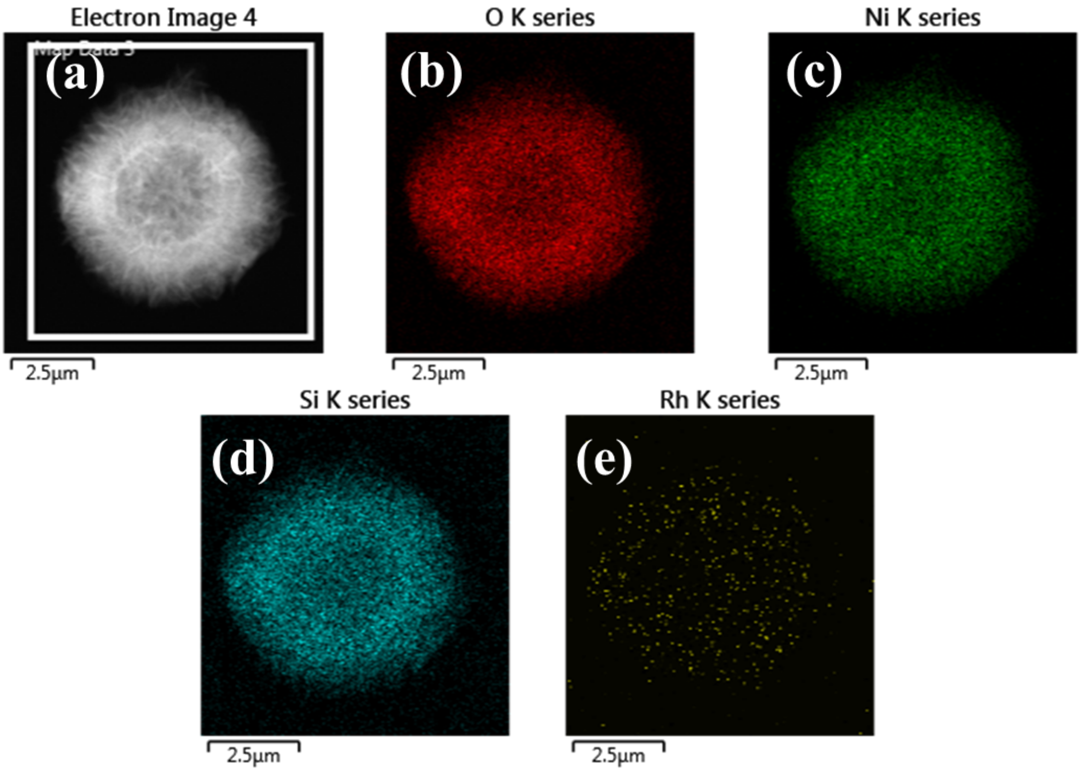

Fig. S7 (a) HAADF-STEM image of Rh/Ni(OH)$_2$@SiO$_2$-3T. EDX elemental mapping images of O (b), Ni (c), Si (d), and Rh (e).

IV. Supplementary References

1. Lee, K. H.; Lee, K. R.; Yi, M. H.; Hur, N. H. *Chem. Commun.*, **2012**, 48, 4414